

*Short Note*Source Uncertainty Estimation in Seismic Intensity
Determination of the Taiwan Region

by Chih-Yih Hsieh, Ting-Li Lin, Yih-Min Wu, and Da-Yi Chen*

Abstract In this work, we quantify the effect of source uncertainties, other than earthquake magnitude and location, in rapid seismic intensity determinations in Taiwan using the strong-motion accelerograms recorded by stations of the Taiwan Strong-Motion Instrumentation Program (TSMIP) between 1991 and 2010. We find that rapid earthquake reporting assumes that a point source has an uncertainty of 0.5° in intensity and 7.2 cm/s^2 in peak ground acceleration (PGA). Therefore, these values can be regarded as the upper bound for precision in the Taiwan rapid reporting system (RRS).

Introduction

Seismic intensity is an indicator that describes the level of ground shaking and the severity of damage at a specific site. By definition, seismic intensity is assessed from the response of people to shaking or from *in-situ* observations of structural damage in the hours or days following a damaging earthquake. For rapid emergency response, such as resource dispatch management, information regarding the spatial distribution of seismic intensity is practically useful, and a near real-time or quick damage assessment in terms of seismic intensity is greatly in demand. One practical way to fulfill this demand is to correlate seismic intensity with peak ground motions because they can be acquired in near real time via a rapid reporting system (RRS).

Taiwan, which is located on the western circum-Pacific seismic belt, is situated in the collision boundary zone between the Philippine Sea plate (PSP) and the Eurasian plate (EP). The entire island of Taiwan is under a northwest-southwest compression with an approximate plate convergence rate of about 8 cm/yr (Yu *et al.*, 1997). As a result, seismicity in Taiwan is considerably high. As the population and the economy grow, Taiwan has been constantly threatened by large, devastating earthquakes, as demonstrated by the catastrophic 1999 Chi-Chi earthquake.

For rapid reporting of felt earthquakes within Taiwan, a real-time strong-motion network, the Taiwan Rapid Earthquake Information Release System (TREIRS), has been operated by the Central Weather Bureau (CWB) since 1997 (Shin *et al.*, 1996; Wu *et al.*, 1997). In addition to routine magnitude and hypocenter determinations following a felt earthquake, peak ground motions that are recorded by the TREIRS system are also used to generate seismic intensity

maps. With over a decade of developments and improvements, the TREIRS system is now integrated into the real-time strong-motion network in Taiwan, which is a part of the rapid reporting system (RRS). The RRS is implemented based on the real-time Central Weather Bureau Seismic Network (CWBSN, Hsiao *et al.*, 2011), and consists of more than 100 digital telemetered seismic stations (Fig. 1).

The rapid estimation of seismic intensity adopted in the RRS is based on the relation between intensity and PGA (Hsu, 1979; Wu *et al.*, 2002), using the following relationship:

$$\log \alpha_I = (I/2) - 0.6, \quad (1)$$

where α_I is acceleration in cm/s^2 and I is the seismic intensity between 0 and 7 (table 1 in Wu *et al.*, 2003). The PGA attenuation relationship (Wu *et al.*, 2001) is used to extrapolate PGA where no instrumental reading is available. The earthquake source parameters involved during the online processing of rapid intensity estimations are earthquake magnitude and location as presented in the attenuation relationship of PGA (Wu *et al.*, 2001). Therefore, for the RRS standard in Taiwan, if two earthquakes with the same magnitude occur at the same place, it is expected that the extrapolated seismic intensity will be the same everywhere. In this study, we investigate the effects of source variations, in addition to magnitude and location, on seismic intensity estimations by analyzing PGA recordings from earthquake pairs with the same magnitudes and locations. For two colocated earthquakes recorded by the same station, the path and site effects are theoretically the same. Therefore, we could define the degree of uncertainty in intensity estimations in the RRS while earthquakes of the same magnitude

*Also at Central Weather Bureau, Taipei 100, Taiwan.

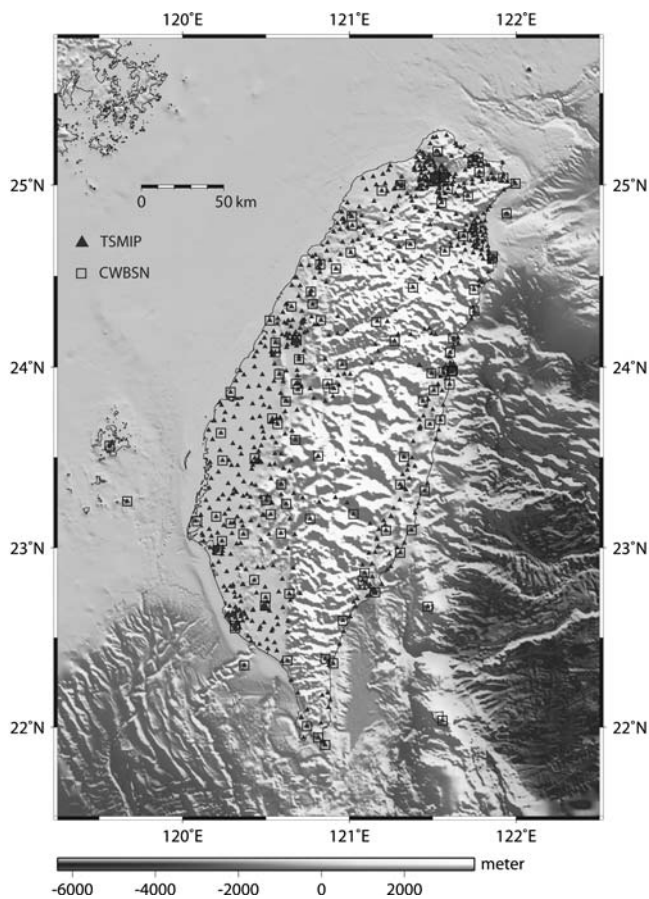


Figure 1. The location of seismic stations of the non-real-time TSMIP (triangles) and the real-time CWBSN (squares) seismic network.

occurred adjacently. In this study, the spatial and temporal distributions of earthquake pairs are also discussed.

Seismic Data

The non-real-time Taiwan Strong-Motion Instrumentation Program (TSMIP) (Liu *et al.*, 1999), operated by the CWB, consists of over 800 free-field stations that are densely distributed throughout the island of Taiwan (Fig. 1). The distribution of the TSMIP seismic stations provides good spatial coverage for earthquake monitoring. Each TSMIP station is equipped with a triaxial, force-balance accelerometer that has a sampling rate of 200 Hz or higher. The network of TSMIP has a station spacing of approximately 5 km throughout the most populated areas, with the exception of high-relief mountain ranges. Because the station density of TSMIP is much higher than that of the CWBSN, earthquake pairs utilized in this study were collected from the TSMIP stations in the period between 1991 and 2010.

The selection criteria for an earthquake pair are as follows: (1) the difference in the epicentral distance is less than 2 km; (2) the difference in the focal depth is less than 2 km; (3) the difference in the magnitude (M_L) is smaller than 0.15.

The cutoff values for each of these criteria are smaller than the corresponding standard deviation or the confidence level in the CWB earthquake catalog. In order to maintain data quality and consistency, all of the PGA readings used in this study are those recorded by 16-bit or higher resolution accelerographs. Measurements recorded by 12-bit accelerographs are not included. To avoid interference of seismic waveforms from two respective events, earthquake pairs with a time interval less than one minute are not included in the analysis. Before applying the selection criteria to the CWB earthquake catalog, we visually checked all of the original accelerograms to remove suspicious waveforms, such as spikelike and steplike waveforms. Finally, a total of 1461 earthquake pairs are selected for this study.

Figure 2 depicts the spatial distributions for all of the studied earthquake pairs along active faults and for damaging events during the study period. In general, the spatial distribution of earthquake pairs is not completely related to the fault surface traces. Two notable concentrated regions of earthquake pairs are observed at the northernmost tip and southern portion of the Longitudinal Valley (LV), which is believed to be a suture zone between the PSP and the EP. At the northernmost LV, densely distributed earthquake pairs are located at depths ranging between 5 and 15 km. The earthquake pairs shown by the green circles in Figure 2 have the highest density and are aggregated into three clusters in space. The region experienced a notable change in the orientation of its maximum horizontal compressive stress axes (S_H) for a depth that ranged between 0 and 20 km (Wu *et al.*, 2010). Wu *et al.* (2010) suggested that the orientation of S_H indicated general agreement with the direction of plate motion between a depth of 0 and 30 km. Little or no earthquake pair is determined in the areas surrounding the epicenters for the 1999 Chi-Chi (M_w 7.6) and the 2010 Jiasian (M_w 6.0) earthquakes.

In the southern portion of the LV, two damaging earthquakes, the 2003 Chengkung (M_w 6.8, depth = 18 km) and the 2006 Taitung (M_w 6.1, depth = 7 km) earthquakes, are located at another notably concentrated region of earthquake pairs. Figure 3 displays the time sequences for earthquake pairs in this concentrated region, along with the two damaging earthquakes. The time sequences suggest that earthquake pairs with focal depths deeper than 14 km are associated with the 2003 Chengkung aftershock sequence. Nevertheless, the 2006 Taitung aftershock sequence does not significantly increase the number of earthquake pairs.

Results

Figure 4 summarizes the distributions of earthquake pairs with respect to their magnitudes, focal depths, and time intervals. The magnitude and focal depth in Figure 4 represent the corresponding average of two events in an earthquake pair, and the time interval is the time difference in the origin times between two events. The maximal magnitude of earthquake pairs is approximately 5.2 (Fig. 4a). As for the

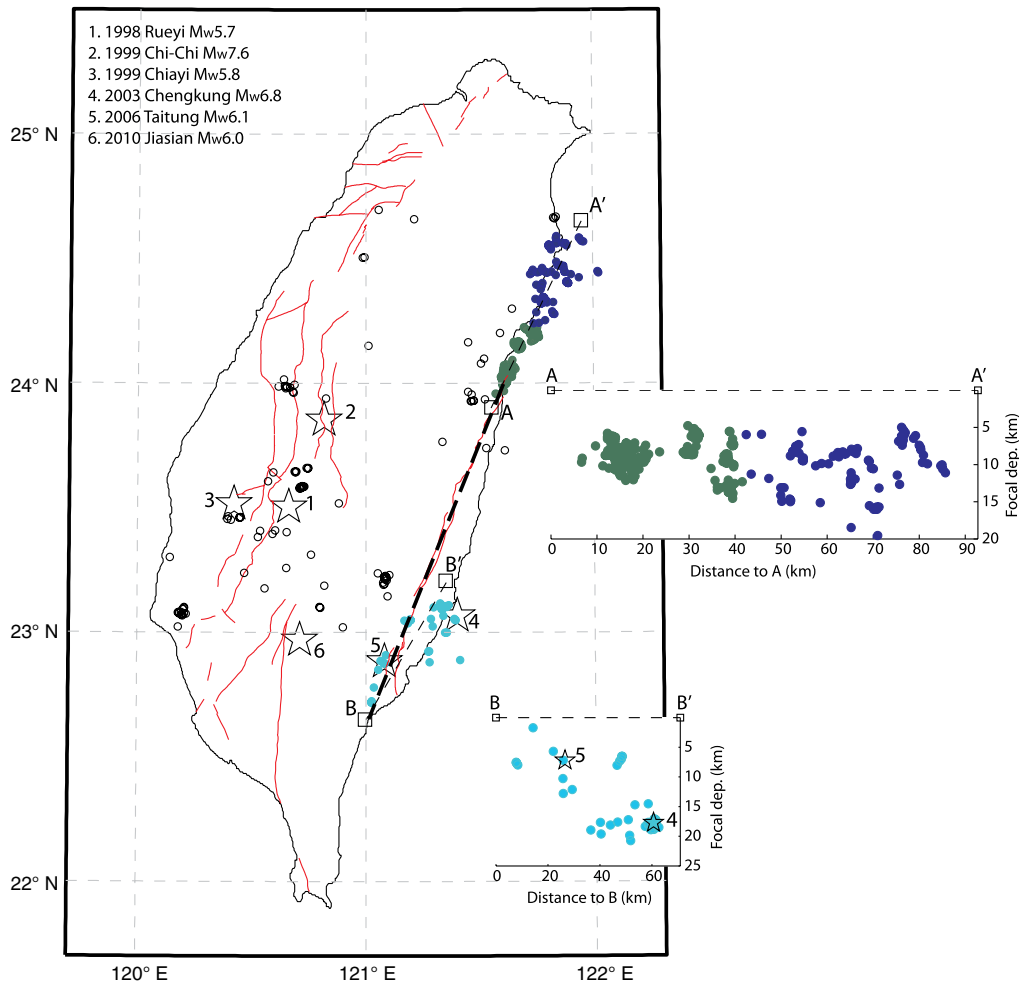


Figure 2. The spatial distribution for all of the studied earthquake pairs, as well as active faults (solid lines) and damaging events (stars) during the study period. The dashed line indicates the trace of the LV. The focal depth distributions along the two profiles (A–A' and B–B') in regions with a high density of earthquake pairs are shown in the insets. The color version of this figure is available only in the electronic edition.

focal depth distribution (Fig. 4b), most earthquake pairs are located at depths of 7 km to 11 km and about 19 km. No earthquake pair is observed at a depth deeper than 22 km. Figure 4c indicates that roughly 50% of the time interval

for earthquake pairs is less than one month, and the longest time interval is approximately 10 years.

Figure 5 shows the PGA residuals, the difference in PGA of two events in the same earthquake pair, as a function of

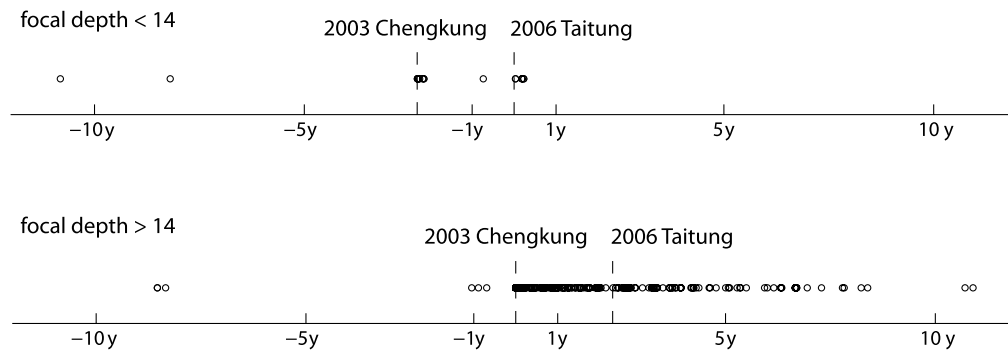


Figure 3. The time sequence of earthquake pairs along the B–B' profiles in Figure 2 at the southern portion of the LV; and the time sequence of the two damaging earthquakes, the 2003 Chengkung (M_w 6.8, depth = 18 km) and the 2006 Taitung (M_w 6.1, depth = 7 km) earthquakes.

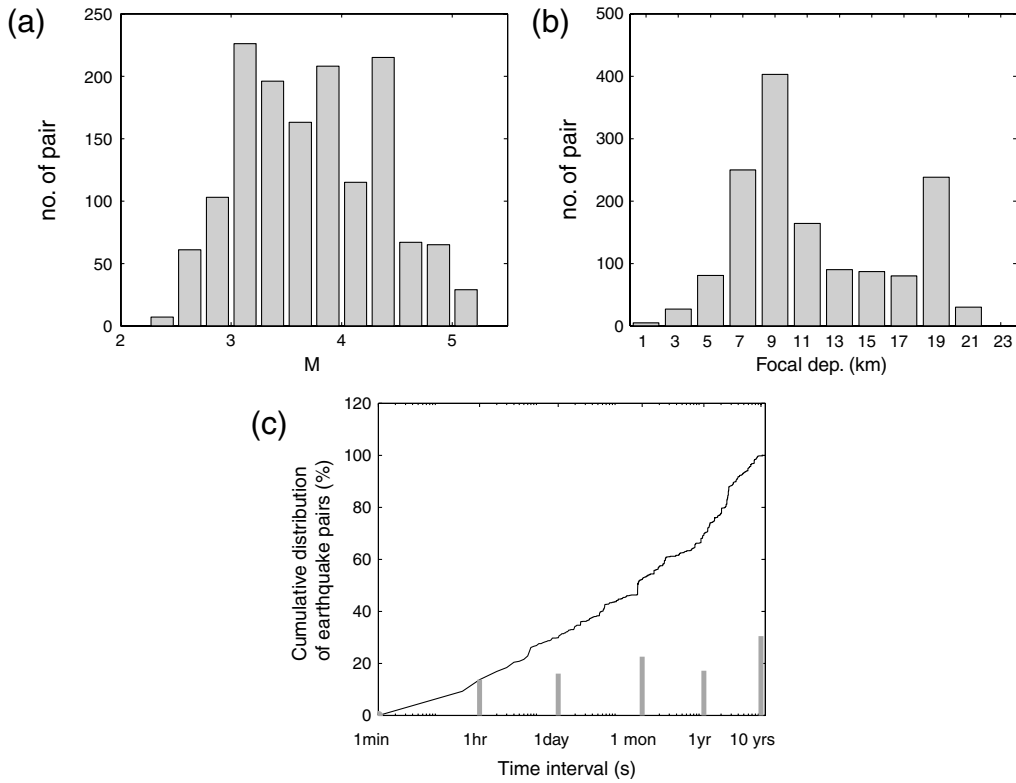


Figure 4. The distributions of earthquake pairs with respect to their (a) average magnitude, (b) average focal depth, and (c) time interval. The gray bars in (c) describe the individual percentage of each time interval, and the line represents the cumulative percentage.

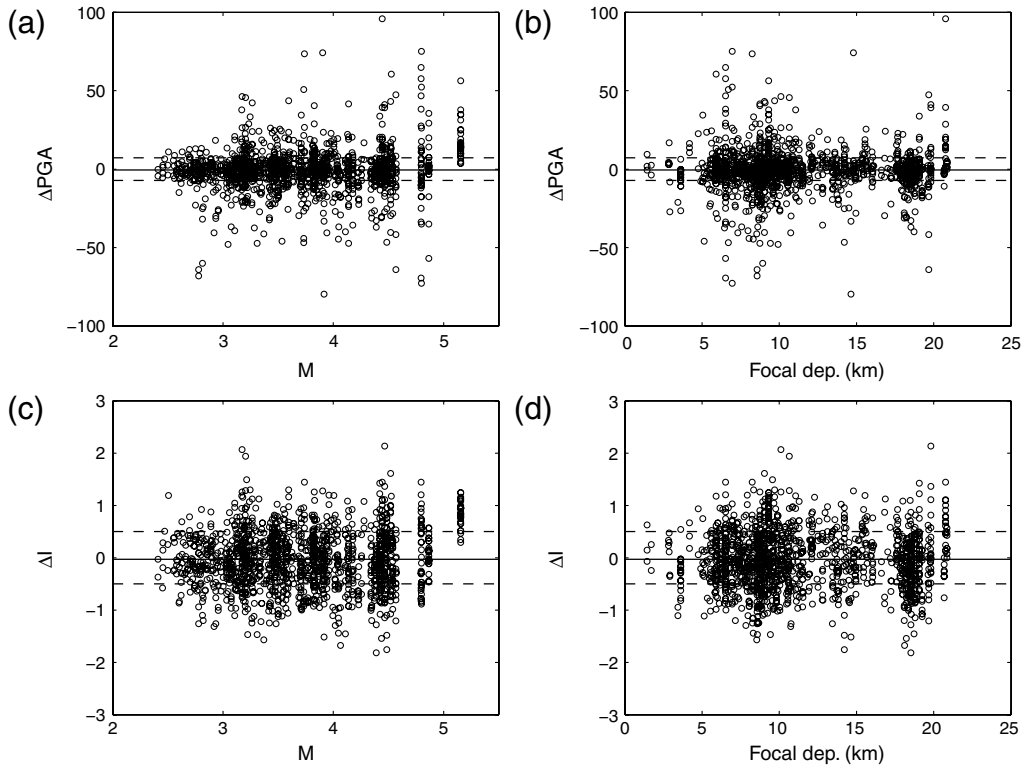


Figure 5. Peak ground acceleration residuals are characterized as a function of (a) magnitude and (b) focal depth. By converting PGA to intensity, we also plotted the intensity residuals (ΔI) as a function of (c) magnitude and (d) focal depth. Solid and dashed lines indicate the mean values and the standard deviations, respectively.

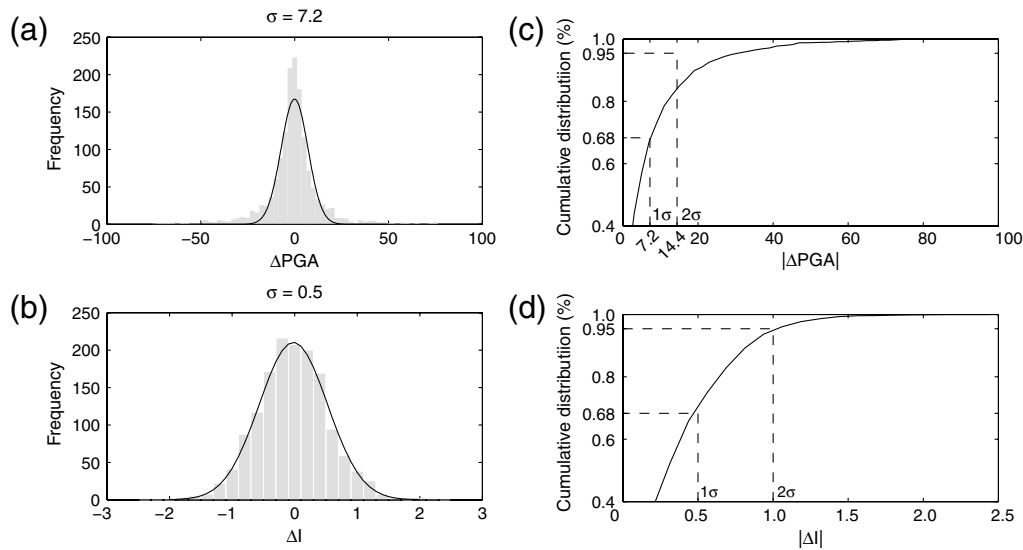


Figure 6. The frequency-residual curves of (a) PGA and (b) intensity. The standard deviations (σ) for the PGA residual and the intensity residual are 7.2 cm/s^2 and 0.5° , respectively. The cumulative distributions are shown for the frequency-residual curves of the (c) PGA residual and the (d) intensity residual.

magnitude (Fig. 5a) and focal depth (Fig. 5b). By applying equation (1), we converted PGA to intensity and plotted the intensity residuals as a function of magnitude (Fig. 5c) and focal depth (Fig. 5d). The general features of Figure 5 suggest that the residuals are randomly, independently, and normally distributed with a mean value close to zero. In Figure 6, the frequency-residual curves of PGA (Fig. 6a) and intensity (Fig. 6b) lead to a consistent conclusion that the residuals are distributed following a Gaussian distribution. The standard deviations (σ) for the PGA and the intensity residuals are, respectively, 7.2 cm/s^2 and 0.5° . Figure 6c,d shows the corresponding cumulative distributions for the frequency-residual curves of PGA (Fig. 6a) and intensity (Fig. 6b), respectively. Following properties for the Gaussian distribution, 68% of both the PGA and the intensity residuals are well within one standard deviation. Ninety-five percent of the PGA residuals are within 28 cm/s^2 , as compared with two standard deviations (14.4 cm/s^2) for a standard Gaussian distribution.

Conclusions

In addition to earthquake magnitude and location, the rapid seismic intensity estimation in Taiwan today does not consider other source variables, such as fault rupture type, direction, duration, and time function. Therefore, at present, the processing of rapid intensity estimations, by assuming a point source, leads to fluctuations introduced by source uncertainties. Our study indicates that fluctuations have a standard deviation of 0.5° in intensity and 7.2 cm/s^2 in PGA. Fluctuations are mainly caused by neglecting the finite fault effects in the process. A value of 0.5° can be regarded as the upper bound for precision in rapid seismic intensity estima-

tions. A fast, comprehensive examination of fault rupturing is necessary for reducing deviations in rapid seismic intensity determinations in Taiwan.

Data and Resources

Raw accelerograms can be accessed by making a request to the Central Weather Bureau, Taiwan. The Generic Mapping Tool software package (Wessel and Smith, 1998) was utilized in this study and is gratefully acknowledged.

Acknowledgments

Our work was supported by the National Science Council (NSC99-2119-175-M-002-022, NSC99-2627-M-002-015, and NSC100-3114-M-002-001) and the Central Weather Bureau. We also thank the Central Weather Bureau for providing the seismic data that were used in this study. We thank two anonymous reviewers for comments that were valuable to the manuscript.

References

- Hsiao, N. C., Y. M. Wu, L. Zhao, D. Y. Chen, W. T. Huang, K. H. Kuo, T. C. Shin, and P. L. Leu (2011). A new prototype system for earthquake early warning in Taiwan, *Soil Dynam. Earthquake Eng.* **31**, no. 2, 201–208, doi [10.1016/j.soildyn.2010.01.008](https://doi.org/10.1016/j.soildyn.2010.01.008).
- Hsu, M. T. (1979). *Seismology*, Lee-Ming Culture Publication Company, Taipei, Taiwan, 16–26 (in Chinese).
- Liu, K. S., T. C. Shin, and Y. B. Tsai (1999). A free-field strong motion network in Taiwan: TSMIP, *Terr. Atmos. Ocean. Sci.* **10**, 377–396.
- Shin, T. C., Y. B. Tsai, and Y. M. Wu (1996). Rapid response of large earthquakes in Taiwan using a real-time telemetered network of digital accelerographs, Paper No. 2137, Presented at the *11th World Conf. of Earthquake Engineering*, Acapulco, Mexico.
- Wessel, P., and W. H. F. Smith (1998). New, improved version of Generic Mapping Tools released, *Eos Trans. AGU* **79**, 579.

- Wu, Y. M., C. C. Chen, T. C. Shin, Y. B. Tsai, W. H. K. Lee, and T. L. Teng (1997). Taiwan Rapid Earthquake Information Release System, *Seismol. Res. Lett.* **68**, 931–943.
- Wu, Y. M., N. C. Hsiao, T. L. Teng, and T. C. Shin (2002). Near real-time seismic damage assessment of the rapid reporting system, *Terr. Atmos. Ocean. Sci.* **13**, 313–324.
- Wu, Y. M., Y. J. Hsu, C. H. Chang, L. S.-Y. Teng, and M. Nakamura (2010). Temporal and spatial variation of stress field in Taiwan from 1991 to 2007: Insights from comprehensive first motion mechanism catalog, *Earth Planet. Sci. Lett.* **298**, 306–316, doi [10.1016/j.epsl.2010.07.047](https://doi.org/10.1016/j.epsl.2010.07.047).
- Wu, Y. M., T. C. Shin, and C. H. Chang (2001). Near real-time mapping of peak ground acceleration and peak ground velocity following a strong earthquake, *Bull. Seismol. Soc. Am.* **91**, 1218–1228.
- Wu, Y. M., T. L. Teng, T. C. Shin, and N. C. Hsiao (2003). Relationship between peak ground acceleration, peak ground velocity and intensity in Taiwan, *Bull. Seismol. Soc. Am.* **93**, 386–396.
- Yu, S. B., H. Y. Chen, L. C. Kuo, S. E. Lallemand, and H. H. Tsien (1997). Velocity field of GPS stations in the Taiwan area, *Tectonophysics* **274**, no. 1–3 41–59.

Department of Geosciences
National Taiwan University
Taipei 10617, Taiwan
(C.-Y.H., Y.-M.W., D.-Y.C.)

Department of Earth Sciences
National Cheng Kung University
No.1, University Road
Tainan City 701, Taiwan
mulas62@gmail.com
(T.-L.L.)

Manuscript received 3 May 2011